scientific reports

Check for updates

OPEN

Establishment and validation of red fox (*vulpes vulpes*) airway epithelial cell cultures at the air-liquid-interface

Andreas W. Oehm[1,2]✉, Blandina I. Oliveira Esteves[3,4], Udo Hetzel[5], Marco P. Alves[3,4,6] & Manuela Schnyder[1,6]

The airway epithelium represents a central barrier against pathogens and toxins while playing a crucial role in modulating the immune response within the upper respiratory tract. Understanding these mechanisms is particularly relevant for red foxes (*Vulpes vulpes*), which serve as reservoirs for various zoonotic pathogens like rabies or the fox tapeworm (*Echinococcus multilocularis*). The study aimed to develop, establish, and validate an air-liquid interface (ALI) organoid model of the fox respiratory tract using primary airway epithelial cells isolated from the tracheas and main bronchi of hunted red foxes. The resulting ALI cultures exhibited a structurally differentiated, pseudostratified epithelium, characterised by ciliated cells, mucus secretion, and tight junctions, as confirmed through histological and immunohistochemical analysis. Functional assessments using a paracellular permeability assay and measurement of transepithelial electrical resistance, demonstrated a tight epithelial barrier. The potential of model's utility for studying innate immune responses to respiratory infections was validated by exposing the cultures to lipopolysaccharide, phorbol-12-myristate-13-acetate and ionomycin, and nematode somatic antigens. Quantitative PCR revealed notable changes in the expression of pro-inflammatory cytokines TNF and IL-33. This in vitro model represents a significant advancement in respiratory research for non-classical species that may act as important wildlife reservoirs for a range of zoonotic pathogens.

Keywords Host-pathogen interaction, Respiratory tract, *In vitro* model, Wildlife reservoir, Fox

The respiratory tract is a critical interface between the environment and the organism, playing a central role in gas exchange and serving as a primary barrier against airborne pathogens, toxins, and other noxious agents. Airway epithelial cells (AEC) proliferate upon epithelial damage and possess crucial roles in initiating, modulating, and guiding downstream immunological responses to pathogens[1–3]. Respiratory viruses such as influenza virus or SARS-CoV-2 primarily infect and replicate in AEC, contributing to disease pathogenesis and clinical outcomes[4,5]. Also, lung infections caused by helminths compromise airway epithelial integrity through the migration of large larvae and the release of biomolecules that interact with the host[6–8]. Understanding these pathogen-airway-epithelium interactions is crucial in a One Health context, as wildlife can serve as reservoirs for a variety of pathogens that impact both human and animal health. Red foxes (*Vulpes vulpes*) are of particular interest due to their widespread presence in rural and urban areas of Europe and their recognised role as reservoirs and vectors of a range of infectious agents. Among the most prominent zoonotic pathogens associated with red foxes are the rabies virus, which although lately controlled in Europe through oral vaccination campaigns, remains a critical concern in regions were control measures are incomplete. Similarly, the detection of SARS-CoV-2 in foxes has raised questions about the role of wildlife as potential reservoirs for emerging zoonoses[9,10]. In addition to viral agents, red foxes carry a plethora of parasitic pathogens of considerable zoonotic concern. Among these, the fox tapeworm (*Echinococcus multilocularis*), responsible for alveolar echinococcosis in humans, and ascarid nematodes such as *Toxocara canis*, are frequently identified in fox populations[13,14]. From a bacterial perspective,

[1]Institute of Parasitology, University of Zurich, Zurich, Switzerland. [2]Graduate School for Cellular and Biomedical Sciences, Bern, Switzerland. [3]Department of Infectious Diseases and Pathobiology, Vetsuisse Faculty, University of Bern, Bern, Switzerland. [4]Institute of Virology and Immunology, Vetsuisse Faculty, Vetsuisse Faculty, University of Bern, Bern, Switzerland. [5]Institute of Veterinary Pathology, Vetsuisse Faculty, University of Zurich, Zurich, Switzerland. [6]Marco P. Alves and Manuela Schnyder contributed equally. ✉email: Andreaswerner.oehm@uzh.ch

foxes are known hosts to *Mycobacterium* spp. and *Salmonella* spp., or coagulase-positive *Staphylococcus* which all can have serious health consequences if transmitted to humans[11,12].We have not reordered number references and citations due to missing citation(s) in manuscript. Please check.Thank you for letting me know. I have provided specifications regaridng the missing informationWe have renumbered the tables in order to maintain sequential order of table citations within text. Please check.Thank you. Pleas make sure that the Figure and Table Legends are included. From what I could see, this information is currently missing in some cases. I have made specifications accordingly throughout the manuscript.

The interactions between pathogens and the fox as a reservoir host remain poorly understood, largely due to the lack of adequate in vitro models. Recent advancements in tissue culture research have led to the development of well-differentiated airway cultures at the air-liquid interface (ALI) that better mimic the upper respiratory tract epithelium, offering a more physiologically relevant platform for studying infectious diseases[15–17], toxicity[18,19], and drug evaluation[20]. These in vitro models, derived from primary tissue, are powerful tools in biomedical research. They replicate key features of their tissue of origin, providing valuable insights into the tissue-specific functions and disease mechanisms. This makes them particularly useful for studying epithelial responses, mucociliary function, and host-pathogen interactions in a more realistic context compared to continuous cell lines and classical submerged culture systems[21,22]. Despite their advantage, well-characterised in vitro models of the respiratory tract derived from carnivores are scarce, which limits our understanding of pathogen interactions with the canid airway epithelium and how these interactions compare with those in other species. To address this gap, the aims of the present study were (I) to develop and validate an ALI in vitro tissue model based on primary AEC from red foxes, (II) to morphologically characterise this model, and (III) to evaluate its suitability for studying innate immune responses to pathogens.

Results

Study subjects

Respiratory epithelial cells were isolated from twelve red foxes (*Vulpes vulpes*) hunted in the Swiss canton of Zurich for population control purposes. Seven of the animals were males and five females. Five animals were older than one year, while seven foxes were younger than one year of age (age was determined according to tooth wear).

Cell count and viability

Primary airway progenitor cells were successfully isolated and cultivated from the tracheal tissue and the main bronchi of twelve individual red foxes. The cells reached confluence within three to five days under submerged conditions and after two to four days on the inserts. Each fox yielded between two to 55.5 million cells (14.5 Mio ± 18.3 Mio), with a viability ranging from 75 to 95.2% (88.3% ±6.2%) illustrated in Fig. 1. When seeding and cultivating cells on the insert, a 100% success rate in the differentiation of the cultures was obtained. Cells could be maintained without considerable degradation for at least three months. Assessment for the presence of *Mycoplasma* spp. revealed that cells from all donors were free from contamination.

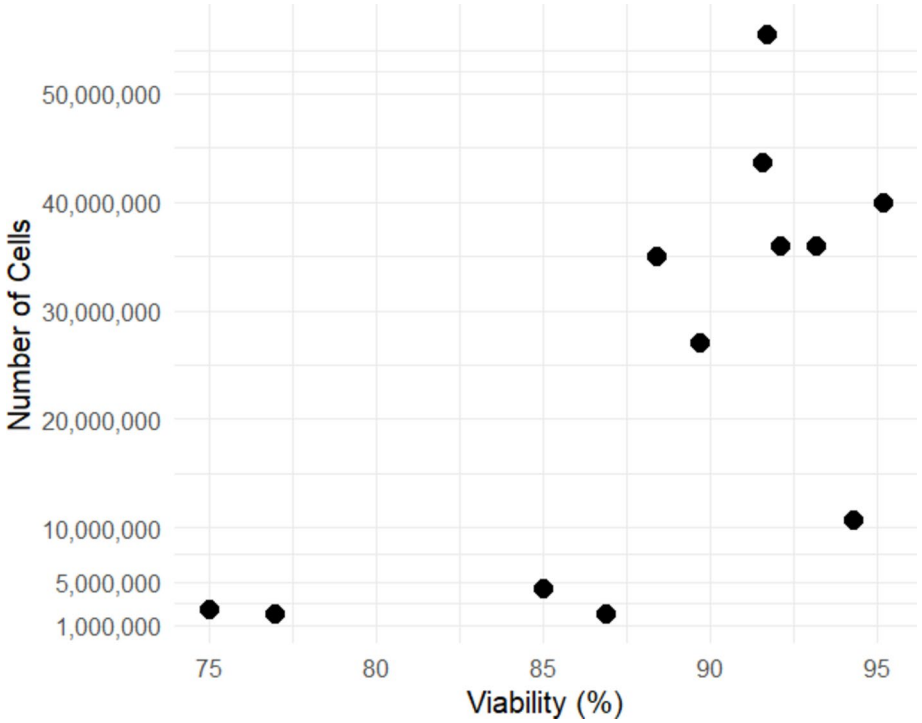

Fig. 1. Scatter plot of number of isolated cells against cell viability in respiratory epithelial cells of twelve foxes.

Histological and immunohistochemical analysis

Haematoxylin-Eosin (HE) stains revealed the structure of a pseudostratified cuboidal/isoprismatic epithelium of closely packed cells that seem to be arranged in layers due to different sizes and different locations of nuclei with a ciliary brush border (Fig. 2a) indicative of a well differentiated respiratory epithelium. Epithelial thickness of in vitro cultures was lower compared to the in vivo situation where cells appeared to be more elongated, high prismatic (Fig. 2b) despite having a similar morphology. Immunohistochemical analysis (Fig. 3) showed well-differentiated AECs (WD-AEC) composed of pancytokeratin-expressing epithelial cells (Fig. 3a) in an intact, organised layer represented by tight junctions (ZO-1, Fig. 3b). Cultures had a consistent, well-formed ciliary brush border (β-tubulin, Fig. 3c) and contained mucus secreting goblet cells (Fig. 3d). The productive secretion of mucus necessitated washing of the cultures once to twice a week.

Epithelial barrier integrity

To assess the barrier integrity of established fox WD-AECs, a paracellular assay for the assessment of epithelial leakage was conducted in triplicate in two independent experiments in all twelve donor foxes. Similarly, TEER was measured in three donors using the chopstick electrode assay. The relative fluorescence in the basolateral chamber was considerably lower in comparison with the reference well, totalling an overall mean leakage of the epithelium of 4.2 ± 0.92% (min 3.0 – max 6.4). TEER was measured to be 2,373.9 ± 756.6 Ωcm^2 (min 1,784 – max 3,673).

Antigen stimulation assay

ALI cultures were exposed to LPS, PMA/ionomycin, and a nematode antigen to their functionality and responsiveness to different antigenic stimuli via the assessment of target gene up-/downregulation. An overview of the results of the stimulation assay are presented in Table 1; Fig. 4. In general, relative TNF expression was less pronounced after 24 h than after four hours. At four hours post stimulation, LPS induced an increase in TNF expression with a fold change of 51.9. PMA/ionomycin was associated with a fold change of 1.6 after four hours, and nematode antigen with a fold change of 3.2. By 24 h post stimulation, the fold increase in TNF expression mounted to 3.2, while PMA/ionomycin and nematode antigen were determined at a fold change of 0.8 each.

Discussion

To study host-pathogen interactions in the airway epithelium, it is essential to use an in vitro model that closely mimics the natural in vivo environment. In particular, this is relevant for species like the red fox, which can serve as important reservoirs for pathogens of zoonotic potential and veterinary significance. However, well differentiated ALI models have been limited for animal species not commonly studied in biomedical research. To address this gap, we describe the development and validation of an ALI in vitro tissue model of the airways using primary tracheal cells derived from red foxes, enhancing our understanding of respiratory biology in this important wildlife reservoir species.

The development of our tissue model involved isolating primary cells from fox respiratory tissues, followed by their expansion and differentiation under ALI conditions. Critical steps included optimising isolation and digestion protocols to ensure high cell viability and fine-tuning conditions that promoted differentiation into a functional airway epithelium. Once these steps were refined, the formation of a fully differentiated epithelium was consistently achieved with a 100% success rate. To our knowledge, information on success rates derived from other wild animal cultures have not been reported in the literature.

Model validation involved comprehensive histological and functional analyses to confirm the presence of key cell types, epithelial barrier integrity, and activation upon exposure to prototype antigens. Post-differentiation morphological and immunohistochemical evaluations of the ALI cultures, using markers indicated by previous work[17], revealed a well-organised pseudostratified columnar epithelium with clearly defined ciliated and mucus-secreting cell populations. Immunostaining further confirmed the expression of epithelial markers, tight junction proteins, and functional ciliary beating, validating both the integrity and functionality of the epithelial layer.

Functional assessments further reinforced the physiological relevance of our system. TEER measurements, consistent with those reported in previous studies in human ALI cultures[23] demonstrated high barrier integrity, with minimal epithelial leakage, both critical parameters for accurately mimicking in vivo conditions. This was

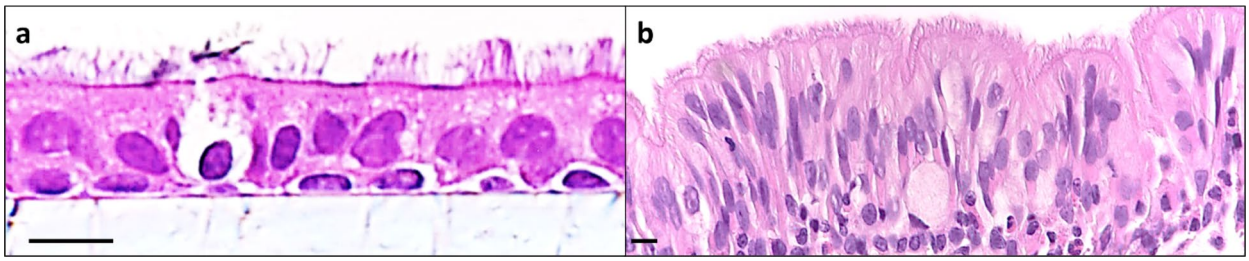

Fig. 2. Red fox primary airway cells maintained at the air-liquid interface present a ciliated pseudostratified columnar epithelium. Representative HE staining of (**a**) three weeks old red fox WD-AECs and (**b**) primary tracheal red fox tissue isolated from afreshly obtained, hunted red fox (Vulpes vulpes) Scale bar: 10 µm; 60x magnification.

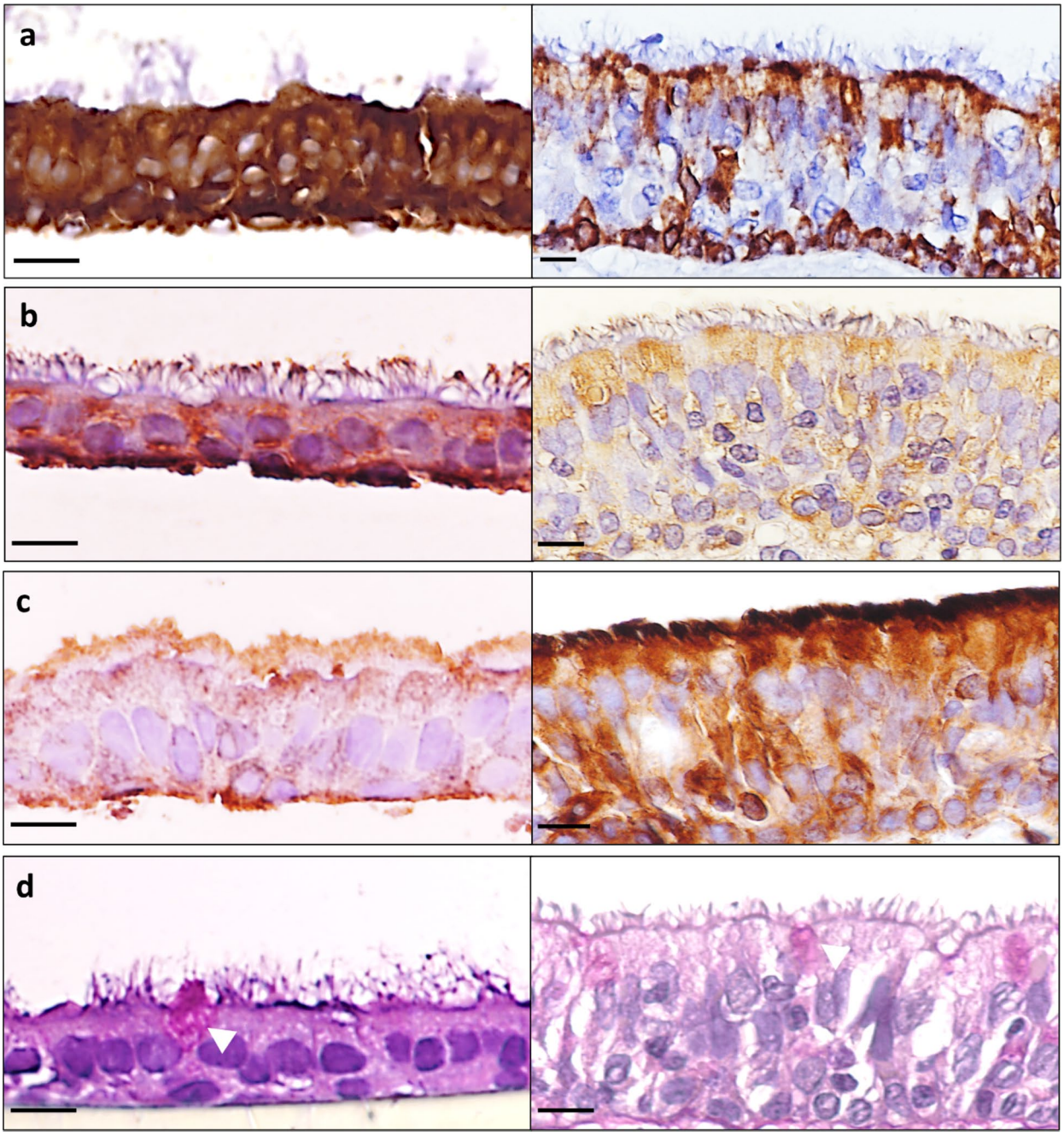

Fig. 3. Differentiated primary red fox well-differentiated airway epithelial cells (left) in comparison to fox primary tracheal tissue (right). (**a**) Immunohistochemical staining of pancytokeratin; (**b**) Immunohistochemical staining of tight junction (ZO-1); (**c**) Immunohistochemical staining of the ciliary brush border (β-tubulin); (**d**) Periodic acid Schiff staining of mucus secreting goblet cells. White arrowhead: mucus-secreting goblet cell. Scale bar: 10 µm; 60x magnification.

further supported by the assessment of epithelial leakage, which showed a low percentage and indicated strong epithelial integrity and tightness. In swine ALI cultures, Wang, et al.[24] have measured the TEER to be as high as 2,100 Ωcm and in human cultures, resistance was determined amount to 2,280 Ωcm^2. In general, TEER values vary between species and depending on the age and passage of the cells[24,26,27]. In the present case, the functional assessments reinforce the relevance and physiological appearance of the fox model.

Antigen stimulation assays provided insights into the immunological responsiveness of the cultures. Differential TNF expression profiles following stimulation with bacterial LPS, PMA/Ionomycin, and nematode somatic antigen over four and 24 h underscored the immunocompetence of our epithelial cell culture model. TNF, a pro-inflammatory cytokine essential for inflammation and immune cell activation[28–30] showed a substantial increase in response to LPS after four hours, suggesting effective recognition of bacterial components.

Gene (Reference)	Primer sequence	Annealing temperature (in °C)
GAPDH[46]	Forward: 5'-GGAGAAAGCTGCCAAATATG-3' Reverse: 5'-ACCAGGAAATGAGCTTGACA-3'	55
TNF[47]	Forward: 5'-CCCCGGGCTCCAGAAGGTG-3' Reverse: 5'-GCAGCAGGCAGAAGAGTGTGGTG-3'	64
IL-33[48]	Forward: 5'-GTACTTTATGCAACTGCGTTCTGG-3' Reverse: 5'-AGACATTGCTTTCTGCACTTTTC-3'	60

Table 1. Sequences of primers for quantitative reverse transcription PCR including cytokine and reference genes:. GAPDH: glyceraldehyde 3-phosphate dehydrogenase; TNF: tumor necrosis factor; IL-33: interleukin 33.

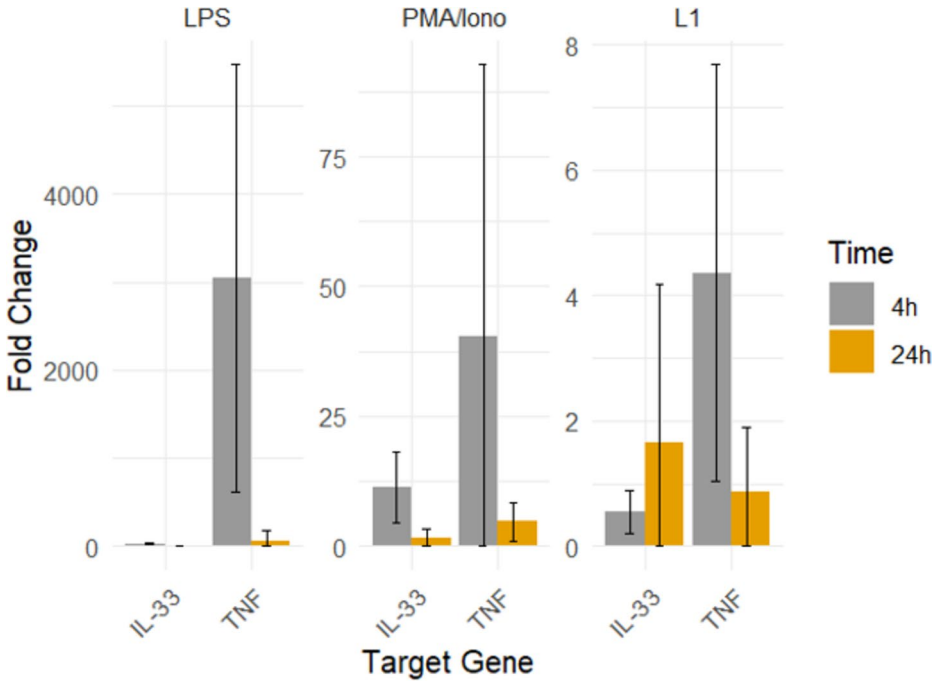

Fig. 4. Expression levels of TNF and IL-33 mRNAs upon stimulation of fox ALI cultures with selected agonists. *LPS* lipopolysaccharide from E. coli; *PMA* phorbol-12-myristat-13-acetat; *Iono* ionomycin, nematode somatic antigen:Angiostrongylus vasorum first-stage larval full somatic antigen. Data from three individual donor foxes.

In contrast, both PMA/Ionomycin and nematode somatic antigen induced a lower TNF expression, indicating an overall weaker or more limited Th1 response, respectively. PMA/Ionomycin is a rather unspecific, broad activator of immune cells[31,32], and parasitic nematodes are commonly encountered by a Th_2-focussed reaction following tissue damage[33–35]. Therefore, the overall lower TNF expression levels after stimulation with PMA/Ionomycin and nematode somatic antigen suggest a potential induction of other pathways. The decline in TNF expression after 24 h across all stimuli aligns with the rapid but transient nature of TNF production[28,30]and suggests potential cellular exhaustion or feedback inhibition. In the case of PMA/ionomycin, the agents can be toxic to cells at prolonged incubation times[36], e.g. 24 h, which could explain the observed lower expression of TNF after 24 h of exposure. Similarly, IL-33, a Th2 cytokine and alarmin constitutively expressed in epithelial and endothelial cells at barrier sites[37–39], displayed varied expression profiles in response to the antigens. LPS triggered a rapid and strong upregulation of IL-33 that decreased over time, indicating a controlled pro-inflammatory response. PMA/ionomycin triggered a moderate initial increase in IL-33 expression that decreased over time as well. Nematode antigen however elicited a delayed upregulation of IL-33 expression, potentially reflecting a role in long-term immune responses to parasitic infections. This delay could be crucial for initiating downstream immunological processes or might suggest parasite interference with the host's immune response.

Despite observing a pseudostratified epithelium with structural and functional differentiation in the ALI system, the cells appeared thinner and shorter compared to the native fox airway epithelium. This discrepancy highlights that in vitro differentiation might not fully recapitulate the complex three-dimensional architecture of the respiratory epithelium, including the subepithelial tissue, microenvironment, and resident cells. In vivo, epithelial cells undergo continuous turnover and differentiation influenced by both intrinsic and extrinsic factors[40,41]. Consequently, the standardised culture conditions of our model cannot fully replicate the dynamic

processes observed in vivo, potentially affecting the morphology and functionality of the cells. To address this, optimisation of culture conditions, along with the use of supportive matrices or co-culture systems, could enhance the ALI model's relevance and robustness.

In summary, primary airway epithelial cultures derived from fox tracheas offer a versatile platform for various applications. These cultures enable detailed investigation into host-pathogen interactions within both veterinary and One-health frameworks. They are also valuable for drug screening and toxicity studies and exploration of respiratory disease mechanisms specific to foxes, whether as wildlife reservoirs or in zoonotic and veterinary contexts. Future efforts should focus on refining the model by integrating immune cells and other components of the respiratory microenvironment, thereby increasing its relevance and utility in biomedical research.

Methods

Ethics statement

Fox primary material was obtained from red foxes hunted in the Swiss canton of Zurich in the context of population control. All methods were carried out in accordance with the relevant Swiss national and cantonal guidelines and regulations for animal experiments and the protection of animals and animal welfare. Foxes were hunted by professionals according to the game law 922.1_1.2.21_119 of the Swiss canton of Zurich and in consent with the responsible supervisor of the corresponding hunting area. Other approvals of experimental protocols by an institutional and/or licensing committee were not required for this study at the time the study was conducted. Methods are reported in accordance with ARRIVE guidelines as applicable to the context of this study (https://arriveguidelines.org).

Isolation of primary fox AEC and establishment of in vitro tissue culture system

Primary fox material was obtained from hunted foxes during hunting season. Tracheas and main bronchi were surgically removed from twelve foxes within six hours after death and placed into ice-cold phosphate-buffered saline (PBS) containing 1% (v/v) 10,000 U/ml penicillin and 10,000 µg/ml streptomycin (Thermo Fisher Scientific, Basel, Switzerland) and 1% (v/v) 250 µg/ml amphotericin B (Thermo Fisher Scientific, Basel, Switzerland). Within two hours after collection, under a sterile bench, the organs were cleaned from connective tissue using surgical material, cut into small pieces of approximately 1 centimeter, and placed into a 50 ml falcon tube containing 45 ml of the digestion solution prepared with DMEM/F12 (Thermo Fisher Scientific, Basel, Switzerland), 0.1% (v/v) protease XIV (1 mg/ml) from *Streptococcus griseus* (Sigma-Aldrich, Buchs, Switzerland), and 0.001% (v/v) DNase I (10 µg/ml; Worthington Biochemical, Lakewood, New Jersey, USA). The digestion process was performed at 4 °C for 2 days with gentle agitation. Enzymatic digestion was stopped by mechanical agitation and by adding 5% (v/v) fetal bovine serum (FBS; FBS Gold, PAN-Biotech, Aidenbach, Germany). The supernatant from the digestion (containing released respiratory progenitor cells) was transferred into a fresh falcon tube and centrifuged at 250 g and 4 °C for eight minutes. The clear fraction was discarded and cells were resuspended in 1 ml DMEM/F12 and counted using a Neubauer chamber. If cell aggregates were observed, the cell suspension was passed through a cell strainer (100 µm). The presence of ciliated cells in the cell pellet indicated a successful digestion.

Fibroblasts were removed by plastic adherence to a plastic petri dish for 4 h (negative selection) and 10,000–20,000 cells/cm^2 were seeded onto a T75 flask coated at room temperature overnight in collagen solution from calf skin (1 mg/ml solution of calf skin collagen in 0.1 M acetic acid (Sigma-Aldrich, Buchs, Switzerland), diluted 1:10 in sterile water and washed twice with sterile PBS). The remainder of the isolated cells was frozen in CryoStor (CryoStor® CS 10, Stemcell Technologies, Vancouver, Canada) as Passage 0. The Submerged culture was conducted at 37 °C and 5% CO_2in a modified expansion medium formulation[17] prepared from PneumaCult™ – Ex medium (Stemcell Technologies, Vancouver, Canada) supplemented with 0.1% % (v/v) hydrocortisone (Stemcell Technologies, Vancouver, Canada), 0.2% (v/v) primocin (InvivoGen, San Diego, CA, USA), 1 µM A83-01 (Tocris Bioscience, Bristol, United Kingdom), 0.2 µM DMH-1 (Stemcell Technologies, Vancouver, Canada), and 0.5 µM CHIR-99,021 (Sigma-Aldrich, Buchs, Switzerland). Once 80–90% confluent under submerged culture conditions, cells were harvested via tryptic digestion (0.25% TrypsinEDTA, TrypLE™ Express Enzyme (1X), no phenol red, Thermo Fisher Scientific, Basel, Switzerland) and transferred into 24-well transparent inserts with a pore size of 0.4 µm (ThinCerts™, Greiner Bio-One, Frickenhausen, Germany) freshly coated overnight at RT with collagen and washed twice with PBS. Cells were seeded at a density of 50,000 cells per insert and both apical and basolateral chambers were filled with modified expansion medium. After the cells reached confluence, the medium was removed from the apical chamber, washed twice with HBSS or PBS or TEER solution and the cultures were maintained under ALI conditions at 37 °C, 5% CO_2, and 95% humidity to promote mucociliary differentiation. Medium in the basolateral chamber was steadily replaced with differentiation medium prepared from PneumaCult™-ALI Medium (Stemcell Technologies, Vancouver, Canada), supplemented with 0.5% (v/v) hydrocortisone (Stemcell Technologies, Vancouver, Canada), 0.2% (v/v) primocin (InvivoGen, San Diego, CA, USA), and 0.2% (v/v) of a 2.0 mg/ml (w/v) heparin solution. Medium was exchanged every second to third day, and cultures were washed weekly after 7 days post-ALI with warm PBS for 20 min at 37 °C. Potential contamination of cultures with *Mycoplasma* spp. was assessed using the *Mycoplasma* gel detection kit (Biotools B&M Labs, Madrid, Spain) according to the manufacturer's instructions.

Morphological evaluation of ALI cultures

Morphological evaluation was performed at passage 1 on material from three representative fox specimens once well-differentiated (WD-ALIs) were observed, usually after 3 weeks in differentiation in ALI culture. Medium from the basolateral chamber was removed and 4% buffered formaldehyde with pH 6.9 (Sigma-Aldrich, Buchs, Switzerland) was added both apically and basolaterally. After fixation for approximately 24 h, cell culture membranes were cut from the insert and routinely embedded in paraffin. Sections of 3.5 µm thickness were

cut and routinely stained with haematoxylin and eosin (HE) to determine the structure of the epithelium. To visualise structural characteristics of respiratory epithelia, immunohistochemical stainings were initiated applying the horseradish peroxidase method using a Dako autostainer (Agilent/Dako, Glostrup, Denmark). Dog and fox tracheas were used as positive controls. Negative controls included the same sections without application of the primary antibody as well as an internal negative control considering non-epithelial cells and tissues of the trachea and adjacent tissues. All employed antibodies were commercially available and showed reactivity to dog antigens, as indicated by the manufacturer's information as well as empirical in-house experience. After deparaffinisation, antigen was retrieved via incubation of the slides with citrate buffer (pH 6.0) at 98 °C for 10 min or with ethylendiamintetraacetic acid (EDTA), pH 9.0) at 98 °C for 20 min. Endogenous peroxidase activity was blocked during an incubation with hydrogen peroxide solution (Dako REAL™ Peroxidase-Blocking Solution, Agilent/Dako, Glostrup, Denmark [S2023]) for ten minutes. Epithelial cells were identified by immunostaining using an antibody targeting pancytokeratin (Lu-5, Agilent/Dako, Glostrup, Denmark [M082101], pretreatment: citrate buffer; dilution 1:50). A polyclonal goat anti-zonula occludens-1 (ZO-1) antibody (Anti-ZO1 tight junction protein antibody - C-terminal; ab190085, Abcam, Cambridge, United Kingdom) directed against the zonula occludens-1 tight junction protein was used to visualise the integrity of the epithelium by staining tight junctions (no pretreatment, dilution 1:300). Staining for β-tubulin using a rabbit monoclonal anti- β tubulin antibody ([EPR16774], ab 179513, Abcam, Cambridge, United Kingdom) targeting β-tubulin was conducted to detect the presence and structure of cilia on ciliated cells (pretreatment: EDTA, dilution 1:400). The Envision-HRP rabbit detection kit (Agilent Technologies, Inc., Santa Clara, CA, USA) was used for all antibodies with a rabbit anti-goat inserted between primary and detection antibody. Periodic Acid-Schiff (PAS) was implemented to visualise mucus secreting goblet cells. For comparative reasons, each immunohistochemical stain of the ALI cultures was accompanied by the same immunohistochemical stain on material from tracheas and main bronchi from red foxes.

Functional evaluation of ALI cultures

Functional evaluation was performed on WD-ALIs after one passage after a minimum of three weeks in culture.

Epithelial barrier integrity

Cell layer integrity test (paracellular assay)

Cell layer integrity was assessed in WD-ALIs of all twelve donor foxes as previously described[42,43]. Specifically, complete PneumaCult™-ALI medium was aspirated from the basolateral chamber and cells were rinsed with phosphate-buffered saline (PBS). A solution containing 2 mg/ml of 4 kDa fluorescein isothiocyanate-dextran (FD4, Sigma-Aldrich, Buchs, Switzerland) in 150 µl of complete PneumaCult™-ALI medium was added apically to the cell cultures. The basolateral chamber was replenished with fresh complete PneumaCult™-ALI medium and the cultures were subsequently incubated in darkness for four hours at 37 °C and 5% CO_2 and 95% humidity. Fluorescence intensity of the basal chamber contents was measured with excitation at 485 nm and emission at 544 nm using a BioTek Synergy H1 microplate reader (Agilent, Santa Clara, CA, USA). Notably, an empty 24-well insert served as the reference value, and fluorescence percentage (=% leakage of the epithelium) was calculated relative to this control.

Transepithelial electrical resistance (TEER)

WD- ALI cultures from three donor foxes underwent PBS washing (10–20 min at 37 °C), followed by addition of 200 µL PBS or TEER solution for 10–20 min to stabilise the temperature. Transepithelial electrical resistance (TEER) was subsequently measured three times using an EVOM[2]meter equipped with STX2 "chopstick" electrodes measuring 4 mm in width and 1 mm in thickness (World Precision Instruments, Florida, USA)[42]. The average resistance value was computed and then adjusted for fluid resistance (insert with no cells) and surface area.

Assessment of functionality via antigen stimulation

WD-ALI cultures of three donor foxes were exposed to lipopolysaccharide solution (5 µg/insert, Thermo Fisher Scientific, Basel, Switzerland), phorbol-12-myristat-13-acetat (PMA, final concentration 10 ng/insert)/ionomycin (final concentration 100 ng/insert) (both from Sigma-Aldrich, Buchs, Switzerland), and 5 µg/insert of nematode antigen of a helminth parasite that would interact with these epithelial cells, i.e. *Angiostrongylus vasorum*first-stage larval (L1) full somatic antigen. All experiments were conducted in duplicate. L1 were isolated from infected fox lungs or from the faeces of infected dogs and foxes via the Baermann funnel method as previously described[44]. Full L1 somatic antigen extracts were prepared by combining L1 with 500 µl of PBS and four stainless steel beads (3 mm diameter, Qiagen, Hilden, Germany). The mixture was processed using the Qiagen TissueLyser II at a frequency of 30 shakes/s for 120 s. The resulting supernatant was transferred to a cryotube and subjected to three freeze-thaw cycles using liquid nitrogen and a water bath at 37 °C. Subsequently, the mixture underwent ultrasonic treatment using a MSE Soniprep 150 (Medical Scientific Equipment MSE, Cholet, France) with an output of 20–30, a duty cycle of 40%, and three cycles of 25 s each, followed by centrifugation at 4 °C and maximum speed for 15 min. The supernatants were then transferred to fresh tubes. Throughout the procedures, parasites and antigens were maintained on ice unless otherwise specified. Protein concentration in the antigen mixtures was quantified using the Pierce™ BCA Protein Assay Kit (Thermo Fisher Scientific, Basel, Switzerland), and aliquots were stored at −80 °C until further use. Prior to the use for cell stimulation, endotoxin levels were detected using the Pierce™ Chromogenic Endotoxin Quant Kit (Thermo Fisher Scientific, Basel, Switzerland). Only antigens with an endotoxin concentration of less than 0.01 ng/ml were used for cell stimulation. To remove endotoxin from samples with an initially higher concentration, the Pierce™ High-Capacity Endotoxin Removal Resin (Thermo Fisher Scientific, Basel, Switzerland) was used.

Gene	Time point after stimulation	Sample	Fold increase ($2^{-\Delta\Delta ct}$ values)
TNF	4 h	LPS	3,041.3 ± 2,427.4
		PMA/ionomycin	40.5 ± 52.2
		Nematode antigen	4.4 ± 3.3
	24 h	LPS	62.5 ± 109.4
		PMA/ionomycin	4.7 ± 3.7
		Nematode antigen	0.9 ± 1.0
IL-33	4 h	LPS	30.0 ± 15.0
		PMA/ionomycin	11.3 ± 6.8
		Nematode antigen	0.6 ± 0.3
	24 h	LPS	0.7 ± 0.6
		PMA/ionomycin	1.6 ± 1.6
		Nematode antigen	1.7 ± 2.5

Table 2. Expression levels of TNF and IL-33 upon stimulation of Fox ALI cultures with selected agonists. LPS: lipopolysaccharide from *E. coli*; PMA: phorbol-12-myristat-13-acetat; nematode antigen: *Angiostrongylus vasorum* first-stage larval full somatic antigen.

Total RNA was isolated after four and 24 h of stimulation using the RNeasy® Mini Kit (Qiagen, Hilden, Germany) following the manufacturer's protocol. Genomic DNA was eliminated using the DNA-free DNA Removal Kit (Thermo Fisher Scientific, Basel, Switzerland). One µg of RNA was mixed with 1 µl of 10x reaction buffer (containing MgCl2) and 1 µl of RNase-free DNase I. Nuclease-free water was added to each tube to reach a final volume of 10 µl. The samples were then incubated at 37 °C for 30 min using a heating block for digestion, followed by inactivation of the DNase at 65 °C for 10 min using the same heating block. Post-DNase treatment, RNA content was reassessed using Nanodrop OneC (Thermo Fisher Scientific, Basel, Switzerland). To generate complementary DNA (cDNA), 250 ng of RNA sample were mixed with 2 µl of 5X Maxima H Minus cDNA Synthesis Master Mix (Thermo Fisher Scientific) and adjusted to a final volume of 10 µl with nuclease-free water. Additionally, to verify the efficacy of the DNase treatment, no-reverse-transcriptase (RT) controls were included for each sample to be used in PCR. Reverse transcription was carried out following the manufacturer's instructions: incubation at 25 °C for 10 min, followed by 50 °C for 25 min, and final denaturation at 85 °C for 5 min.

For qPCR analysis, PowerUp SYBR Green Master Mix (Applied Biosystems, Zurich, Switzerland) was employed. Each reaction mixture consisted of 1 µl of 1:5 diluted cDNA, along with 1 µM of both forward and reverse primers (Microsynth, Balgach, Switzerland), prepared according to the manufacturer's guidelines. The primers were further diluted 1:100 with nuclease-free water to attain a PCR working concentration of 1 µM. AlI cultures were examined for the expression of TNF and IL-33 (Table 2). Canine glyceraldehyde 3-phosphate dehydrogenase (GAPDH) served as the housekeeping gene and internal control. Additionally, duplicate no-template-controls (NTCs), comprising only the master mix and 1 µl of nuclease-free water were included to monitor potential contamination. Amplification was carried out using the QuantStudio 7 Flex system (Applied Biosystems, Zurich, Switzerland) and MicroAmp optical 96-well reaction plates (Applied Biosystems, Zurich, Switzerland). qPCR for GAPDH consisted of a hold stage (50 °C 2 min, 95 °C 2 min), followed by 40 cycles of PCR reaction (95 °C 15 s, 55 °C 15s, 72 °C 1 min), an/d a melt curve stage (95 °C for 15 s, 60 °C for 1 min, 95 °C for 15 s). For TNF, the hold stage covered 50 °C 2 min, 95 °C 2 min, followed by 40 cycles of 95 °C 15 s, 64 °C 1 min, 72 °C 1 min, and a melt curve stage (95 °C for 15 s, 60 °C for 1 min, 95 °C for 15 s). For IL-33, qPCR covered a hold stage of 95 °C for 10 s, followed by 40 cycles of PCR reaction (95 °C for 5 s and 60 °C for 30 s) and the melt curve stage (95 °C for 15 s, 60 °C for 1 min, 95 °C for 15 s). The delta-delta Ct method was applied to calculate the relative fold gene expression[45]. Plots and data visualisations were created using R Software for Statistical Computing, version 4.3.2[49].

Data availability

The data supporting the results and conclusions of this article are included in the manuscript. Raw data files are available upon request to the corresponding author.

Received: 15 October 2024; Accepted: 11 March 2025
Published online: 22 March 2025

References

1. Hewitt, R. J. & Lloyd, C. M. Regulation of immune responses by the airway epithelial cell landscape. *Nat. Rev. Immunol.* **21**, 347–362. https://doi.org/10.1038/s41577-020-00477-9 (2021).
2. Fehrenbach, H. Alveolar epithelial type II cell: defender of the alveolus revisited. *Respir Res.* **2**, 33–46. https://doi.org/10.1186/rr36 (2001).
3. Kato, A. & Schleimer, R. P. Beyond inflammation: airway epithelial cells are at the interface of innate and adaptive immunity. *Curr. Opin. Immunol.* **19**, 711–720. https://doi.org/10.1016/j.coi.2007.08.004 (2007).

4. Jin, Y. et al. Virology, Epidemiology, Pathogenesis, and Control of COVID-19. *Viruses* 12 (2020). https://doi.org/10.3390/v12040372
5. Shin, D. L. et al. Avian influenza A virus infects swine airway epithelial cells without prior adaptation. *Viruses* **12** https://doi.org/10.3390/v12060589 (2020).
6. Schnyder, M. et al. Clinical, laboratory and pathological findings in dogs experimentally infected with *Angiostrongylus vasorum*. *Parasitol. Res.* **107**, 1471–1480. https://doi.org/10.1007/s00436-010-2021-9 (2010).
7. Gillis-Germitsch, N., Kockmann, T., Asmis, L. M., Tritten, L. & Schnyder, M. The *Angiostrongylus vasorum* excretory/secretory and surface proteome contains putative modulators of the host coagulation. *Front. Cell. Infect. Microbiol.* **11**, 753320. https://doi.org/10.3389/fcimb.2021.753320 (2021).
8. Schwartz, E., Rozenman, J. & Perelman, M. Pulmonary manifestations of early schistosome infection among nonimmune travelers. *Am. J. Med.* **109**, 718–722. https://doi.org/10.1016/s0002-9343(00)00619-7 (2000).
9. Porter, S. M., Hartwig, A. E., Bielefeldt-Ohmann, H., Bosco-Lauth, A. M. & Root, J. J. Susceptibility of wild Canids to SARS-CoV-2. *Emerg. Infect. Dis.* **28**, 1852–1855. https://doi.org/10.3201/eid2809.220223 (2022).
10. Nouvellet, P. et al. Rabies and canine distemper virus epidemics in the red Fox population of Northern Italy (2006–2010). *PLoS One*. **8**, e61588. https://doi.org/10.1371/journal.pone.0061588 (2013).
11. Michelet, L. et al. *Mycobacterium Bovis* infection of red Fox, France. *Emerg. Infect. Dis.* **24**, 1150–1153. https://doi.org/10.3201/eid2406.180094 (2018).
12. Nowakiewicz, A. et al. Free-Living species of carnivorous mammals in Poland: red Fox, Beech Marten, And raccoon as a potential reservoir of Salmonella, Yersinia, Listeria spp. And Coagulase-Positive Staphylococcus. *PLoS One*. **11**, e0155533. https://doi.org/10.1371/journal.pone.0155533 (2016).
13. Deplazes, P., Hegglin, D., Gloor, S. & Romig, T. Wilderness in the City: the urbanization of *Echinococcus multilocularis*. *Trends Parasitol.* **20**, 77–84. https://doi.org/10.1016/j.pt.2003.11.011 (2004).
14. Otranto, D. & Deplazes, P. Zoonotic nematodes of wild carnivores. *Int. J. Parasitol. Parasites Wildl.* **9**, 370–383. https://doi.org/10.1016/j.ijppaw.2018.12.011 (2019).
15. Meng, F., Wu, N. H., Seitz, M., Herrler, G. & Valentin-Weigand, P. Efficient suilysin-mediated invasion and apoptosis in Porcine respiratory epithelial cells after Streptococcal infection under air-liquid interface conditions. *Sci. Rep.* **6**, 26748. https://doi.org/10.1038/srep26748 (2016).
16. Wu, N. H. et al. The differentiated airway epithelium infected by influenza viruses maintains the barrier function despite a dramatic loss of ciliated cells. *Sci. Rep.* **6**, 39668. https://doi.org/10.1038/srep39668 (2016).
17. Shin, D. L. et al. Overcoming the Barrier of the Respiratory Epithelium during Canine Distemper Virus Infection. *mBio* 13, e0304321 (2022). https://doi.org/10.1128/mbio.03043-21
18. Paur, H. R. et al. In-vitro cell exposure studies for the assessment of nanoparticle toxicity in the lung—A dialog between aerosol science and biology. *J. Aerosol Sci.* **42**, 668–692 (2011).
19. Lacroix, G. et al. Air-Liquid interface in vitro models for respiratory toxicology research: consensus workshop and recommendations. *Appl. Vitro Toxicol.* **4**, 91–106. https://doi.org/10.1089/aivt.2017.0034 (2018).
20. Lin, H. et al. Air-liquid interface (ALI) culture of human bronchial epithelial cell monolayers as an in vitro model for airway drug transport studies. *J. Pharm. Sci.* **96**, 341–350. https://doi.org/10.1002/jps.20803 (2007).
21. Pezzulo, A. A. et al. The air-liquid interface and use of primary cell cultures are important to recapitulate the transcriptional profile of in vivo airway epithelia. *Am. J. Physiol. Lung Cell. Mol. Physiol.* **300**, L25–31. https://doi.org/10.1152/ajplung.00256.2010 (2011).
22. Prytherch, Z. et al. Tissue-Specific stem cell differentiation in an in vitro airway model. *Macromol. Biosci.* **11**, 1467–1477. https://doi.org/10.1002/mabi.201100181 (2011).
23. Yoo, J. W. et al. Serially passaged human nasal epithelial cell monolayer for in vitro drug transport studies. *Pharm. Res.* **20**, 1690–1696. https://doi.org/10.1023/a:1026112107100 (2003).
24. Wang, H. et al. Establishment and comparison of air-liquid interface culture systems for primary and immortalized swine tracheal epithelial cells. *BMC Cell. Biol.* **19**, 10. https://doi.org/10.1186/s12860-018-0162-3 (2018).
25. Xu, W. et al. A novel method for pulmonary research: assessment of bioenergetic function at the air–liquid interface. *Redox Biol.* **2**, 513–519 (2014).
26. Min, K. A., Rosania, G. R. & Shin, M. C. Human airway primary epithelial cells show distinct architectures on membrane supports under different culture conditions. *Cell. Biochem. Biophys.* **74**, 191–203. https://doi.org/10.1007/s12013-016-0719-8 (2016).
27. Stewart, C. E., Torr, E. E., Jamili, M., Bosquillon, N. H. & Sayers, I. C. Evaluation of differentiated human bronchial epithelial cell culture systems for asthma research. *J Allergy (Cairo)* 943982 (2012). (2012). https://doi.org/10.1155/2012/943982
28. Fong, Y. et al. Antibodies to cachectin/tumor necrosis factor reduce Interleukin 1 beta and Interleukin 6 appearance during lethal bacteremia. *J. Exp. Med.* **170**, 1627–1633. https://doi.org/10.1084/jem.170.5.1627 (1989).
29. Jin, P. et al. Interferon-γ and tumor necrosis Factor-α polarize bone marrow stromal cells uniformly to a Th1 phenotype. *Sci. Rep.* **6**, 26345. https://doi.org/10.1038/srep26345 (2016).
30. Jordan, S. J. et al. The predominant CD4(+) Th1 cytokine elicited to *Chlamydia trachomatis* infection in women is tumor necrosis factor alpha and not interferon gamma. *Clin. Vaccine Immunol.* **24** https://doi.org/10.1128/cvi.00010-17 (2017).
31. Wan, S. et al. Costimulation molecules differentially regulate the ERK-Zfp831 axis to shape T follicular helper cell differentiation. *Immunity* **54**, 2740–2755e2746. https://doi.org/10.1016/j.immuni.2021.09.018 (2021).
32. Lee, J. H. et al. Single-cell RNA sequencing identifies distinct transcriptomic signatures between PMA/ionomycin- and αCD3/αCD28-activated primary human T cells. *Genomics Inf.* **21**, e18. https://doi.org/10.5808/gi.23009 (2023).
33. Mohrs, K., Harris, D. P., Lund, F. E. & Mohrs, M. Systemic dissemination and persistence of Th2 and type 2 cells in response to infection with a strictly enteric nematode parasite. *J. Immunol.* **175**, 5306–5313. https://doi.org/10.4049/jimmunol.175.8.5306 (2005).
34. Oser, L. et al. *Ascaris suum* infection in juvenile pigs elicits a local Th2 response in a setting of ongoing Th1 expansion. *Front. Immunol.* **15**, 1396446. https://doi.org/10.3389/fimmu.2024.1396446 (2024).
35. Gerbe, F. et al. Intestinal epithelial tuft cells initiate type 2 mucosal immunity to helminth parasites. *Nature* **529**, 226–230. https://doi.org/10.1038/nature16527 (2016).
36. Olsen, I. & Sollid, L. M. Pitfalls in determining the cytokine profile of human T cells. *J. Immunol. Methods*. **390**, 106–112. https://doi.org/10.1016/j.jim.2013.01.015 (2013).
37. Pascual-Reguant, A. et al. T(H)17 cells express ST2 and are controlled by the alarmin IL-33 in the small intestine. *Mucosal Immunol.* **10**, 1431–1442. https://doi.org/10.1038/mi.2017.5 (2017).
38. Tan, W. et al. Interleukin-33-Dependent accumulation of regulatory T cells mediates pulmonary epithelial regeneration during acute respiratory distress syndrome. *Front. Immunol.* **12**, 653803. https://doi.org/10.3389/fimmu.2021.653803 (2021).
39. Moussion, C., Ortega, N. & Girard, J. P. The IL-1-like cytokine IL-33 is constitutively expressed in the nucleus of endothelial cells and epithelial cells in vivo: a novel 'alarmin'? *PLoS One*. **3**, e3331. https://doi.org/10.1371/journal.pone.0003331 (2008).
40. Hong, K. U., Reynolds, S. D., Watkins, S., Fuchs, E. & Stripp, B. R. Basal cells are a multipotent progenitor capable of renewing the bronchial epithelium. *Am. J. Pathol.* **164**, 577–588. https://doi.org/10.1016/s0002-9440(10)63147-1 (2004).
41. Rawlins, E. L., Clark, C. P., Xue, Y. & Hogan, B. L. The Id2 + distal tip lung epithelium contains individual multipotent embryonic progenitor cells. *Development* **136**, 3741–3745. https://doi.org/10.1242/dev.037317 (2009).
42. Schögler, A. et al. Characterization of pediatric cystic fibrosis airway epithelial cell cultures at the air-liquid interface obtained by non-invasive nasal cytology brush sampling. *Respir Res.* **18**, 215. https://doi.org/10.1186/s12931-017-0706-7 (2017).

43. Vielle, N. J. et al. The human upper respiratory tract epithelium is susceptible to flaviviruses. *Front. Microbiol.* **10**, 811. https://doi.org/10.3389/fmicb.2019.00811 (2019).
44. Oehm, A. W. & Schnyder, M. Adult parasite burden and excretion of first-stage larvae of Angiostrongylus vasorum in dogs: methodologically relevant diagnostic aspects and associations with serological detection of parasite antigen and specific antibodies. *Vet. Parasitol.* **312**, 109814. https://doi.org/10.1016/j.vetpar.2022.109814 (2022).
45. Livak, K. J. & Schmittgen, T. D. Analysis of relative gene expression data using real-time quantitative PCR and the 2(-Delta delta C(T)) method. *Methods* **25**, 402–408. https://doi.org/10.1006/meth.2001.1262 (2001).
46. Park, E. S., Uchida, K., Nakayama, H. & Th1- Th2-, and Th17-related cytokine and chemokine receptor mRNA and protein expression in the brain tissues, T cells, and macrophages of dogs with necrotizing and granulomatous meningoencephalitis. *Vet. Pathol.* **50**, 1127–1134. https://doi.org/10.1177/0300985813488957 (2013).
47. Veenhof, E. Z., Rutten, V. P., van Noort, R., Knol, E. F. & Willemse, T. Evaluation of T-cell activation in the duodenum of dogs with cutaneous food hypersensitivity. *Am. J. Vet. Res.* **71**, 441–446. https://doi.org/10.2460/ajvr.71.4.441 (2010).
48. Asahina, R., Nishida, H., Kamishina, H. & Maeda, S. Expression of IL-33 in chronic lesional skin of canine atopic dermatitis. *Vet. Dermatol.* **29**, 246–e291. https://doi.org/10.1111/vde.12531 (2018).
49. R Core Team. R: A Language and environment for statistical computing. *R Foundation Stat. Comput. Vienna, Austria*. https://www.R-project.org/ (2023).

Acknowledgements

We wish to cordially thank (in alphabetical order of their surnames) Nadine Garcia, Barbara Praehauser, and Sabina Wunderlin-Giuliani for outstanding technical assistance. This study received financial support from the Foundation for Research in Science and the Humanities at the University of Zurich, grant number STWF-23-012 and the Swiss National Science Foundation (Grant No: 310030_201045/1).

Author contributions

AOE, MPA, and MS designed the study; AOE conducted the fox dissections, collected the materials and performed the experiments together with BOE and UH; AOE, BOE, UH, MPA, and MS analysed the data; AOE write the manuscript with contributions from all authors.

Declarations

Competing interests

The authors declare no competing interests.

Additional information

Correspondence and requests for materials should be addressed to A.W.O.

Reprints and permissions information is available at www.nature.com/reprints.

Publisher's note Springer Nature remains neutral with regard to jurisdictional claims in published maps and institutional affiliations.